Environmental Pollution 248 (2019) 238–246

Contents lists available at ScienceDirect

Environmental Pollution

journal homepage: www.elsevier.com/locate/envpol

Indirect N_2O emissions from groundwater under high nitrogen-load farmland in eastern China☆

Wei Zhou [a, b], Jinghui Lin [a, b], Quan Tang [a], Zhijun Wei [a], Graeme Schwenke [c], De Li Liu [d, e], Xiaoyuan Yan [a, b, *]

[a] State Key Laboratory of Soil and Sustainable Agriculture, Institute of Soil Science, Chinese Academy of Sciences, Nanjing, 210008, China
[b] Changshu Agro-ecological Experimental Station, Chinese Academy of Sciences, Changshu, 215555, China
[c] NSW Department of Primary Industries, 4 Marsden Park Road, Tamworth, NSW, 2340, Australia
[d] NSW Department of Primary Industries, Wagga Wagga Agricultural Institute, Wagga Wagga, NSW, 2650, Australia
[e] Climate Change Research Centre and ARC Centre of Excellence for Climate Extremes, University of New South Wales, Sydney, NSW, 2052, Australia

ARTICLE INFO

Article history:
Received 13 October 2018
Received in revised form
10 January 2019
Accepted 11 February 2019
Available online 13 February 2019

Keywords:
Indirect N_2O emission
Land-use type
Denitrification
EF_{5g}
Groundwater

ABSTRACT

Current estimates of global indirect N_2O emissions are based on a relatively small dataset and remain a major source of uncertainly in the global N_2O budget. Nitrogen (N)-enriched groundwater from agricultural fields may act as an important source of indirect N_2O emissions as it discharges to adjacent watershed areas. During 2015–2017, dissolved N_2O concentrations in groundwater were measured and indirect N_2O emission factors (EF_{5g}) calculated under three typical high-N land-use types (vineyard, vegetable field and paddy field) in eastern China. The average dissolved N_2O concentrations in groundwater were 58.1 ± 40.4, 18.5 ± 11.5 and 0.72 ± 0.27 μg N L^{-1} for vineyard, vegetable field and paddy field, respectively. The dissolved N_2O was over-saturated and was therefore a net source of N_2O to the atmosphere. The indirect N_2O emission factors (EF_{5g}) of vineyard (0.0091) and vegetable (0.0092) fields were much higher than the current Intergovernmental Panel on Climate Change (IPCC) default value of 0.0025 which indicated that these land-uses may have led to indirect N_2O emissions from the underlying groundwater. In contrast, the EF_{5g} of the paddy field (0.0019) was slightly lower than the default EF_{5g} proposed by IPCC (2006) and contributed minimal indirect N_2O emissions to the atmosphere. However, the current IPCC method may have overestimated the contribution of groundwater N_2O to the global N cycle because it took residual but not initial groundwater NO_3^--N concentration into account when calculating EF_{5g}. Therefore, we proposed the adoption of an improved method for calculating the EF_{5g} and compared it to the current IPCC (2006) method using data from the present study and other published data. The results of the comparison showed that the improved method was more scientifically appropriate measurement for calculating EF_{5g}.

© 2019 Elsevier Ltd. All rights reserved.

1. Introduction

Nitrous oxide (N_2O) is a powerful greenhouse gas for its 298 times greater global warming potential than carbon dioxide (CO_2) over a 100-year timescale (Myhre et al., 2013). It contributes 6% of the total anthropogenic radioactive forcing at current concentration (Stocker, 2014). N_2O is also the primary anthropogenic stratospheric ozone (O_3) depleting substance for its role in the catalytic reduction of O_3 to oxygen (O_2) (Ravishankara et al., 2009). The concentration of N_2O in the atmosphere has increased at an annual rate of 0.75 ppb yr^{-1} since the late 1970s (Stocker, 2014).

Current estimates of the total annual global flux of N_2O into the atmosphere are 18.8 Tg N yr^{-1}, with 45% of this derived from anthropogenic sources (Syakila and Kroeze, 2011). Agriculture is the largest anthropogenic source of N_2O (5.3–8.0 Tg N yr^{-1}) which is made up of (i) direct N_2O emissions from soil (1.8–2.1 Tg N yr^{-1}) and animal production (2.1–2.3 Tg N yr^{-1}), and (ii) indirect N_2O emissions (1.3–2.6 Tg N yr^{-1}) from aquatic areas adjacent to agricultural fields such as rivers, lakes, wetlands and groundwater (Cooper et al., 2017; Ma et al., 2018).

It is currently estimated that about 73% (0.6–1.9 Tg N yr^{-1}) of

☆ This paper has been recommended for acceptance by Dr. Haidong Kan.

* Corresponding author. State Key Laboratory of Soil and Sustainable Agriculture, Institute of Soil Science, Chinese Academy of Sciences, Nanjing, 210008, China.
E-mail address: yanxy@issas.ac.cn (X. Yan).

https://doi.org/10.1016/j.envpol.2019.02.027
0269-7491/© 2019 Elsevier Ltd. All rights reserved.

indirect N_2O emissions are sourced from N leaching and runoff (Cooper et al., 2017; Reay et al., 2012; Reay et al., 2003) and N-enriched groundwater has recently been reported to be an important source of indirect N_2O emissions (Jurado et al., 2017; Tian et al., 2018). Contamination of the groundwater below agricultural fields by reactive N (mainly nitrate, NO_3^--N) is widespread due to the high N fertilizer loading applied to these fields (Gu et al., 2013; Weymann et al., 2008; Xing et al., 2002; Zhou et al., 2016). High concentrations of NO_3^--N in the groundwater, combined with anaerobic conditions, lead to denitrification (Rivett et al., 2008). Therefore, groundwater with a high NO_3^--N concentration is often over-saturated with N_2O, an obligate intermediate product of denitrification, in relation to the atmospheric N_2O equilibrium in aquifers (Jurado et al., 2017). The N_2O in groundwater is transferred to the atmosphere during well pumping or natural discharge to oceans, wetlands, rivers and lakes (Hasegawa et al., 2000; Jahangir et al., 2012). Therefore, groundwater discharges represent a mixture of N_2O from different aquifers and may be an important source of N_2O to the atmosphere from watershed areas (Fox et al., 2014; Gardner et al., 2016).

The Intergovernmental Panel on Climate Change (IPCC) uses emission factors to estimate indirect N_2O emissions from N leaching and runoff (EF_5) (IPCC, 2006). The EF5 is further subdivided into three subcategories :

$$EF_5 = EF_{5g}\,(0.0025) + EF_{5r}\,(0.0025) + EF_{5e} \qquad (0.0025)$$

where EF_{5g} is the emission factor for groundwater, EF_{5r} is the emission factor for rivers and EF_{5e} is the emission factor for estuarine coastal areas. The IPCC defines EF_{5g} as either (i) the ratio between N_2O emission to the atmosphere (N_2O-N_{out}) and nitrogen (N) input to the system (Total N_{input}), or (ii) the ratio of dissolved N_2O to NO_3^--N in the water body. As many studies often lack information of N_2O emissions and total N-input of the groundwater, most EF_{5g} data reported in the literature has been derived from the ratio of dissolved N_2O to NO_3^--N in groundwater (Jurado et al., 2017).

Research on EF_{5g} measurements has increased since the IPCC (2006) guidelines but has been limited in scope and highly variable, with results ranging from 0.00002 to 0.73 (Jurado et al., 2017; Tian et al., 2019). Therefore, the default value of EF_{5g} remains poorly supported by research data and is a major source of uncertainly in the global N_2O budget (Cooper et al., 2017). Furthermore, the default EF_{5g} has been broadly criticized for either significantly over- or under-estimating actual groundwater-based N_2O emissions (Jahangir et al., 2013; McAleer et al., 2017; Tian et al., 2019; Weymann et al., 2008; Zhou et al., 2017).

In addition to the large uncertainty surrounding actual EF_{5g} values, there are also limitations in the methods used for estimating indirect N_2O emission because they assume that the aquatic systems act solely as a domain of transport without any internal conversion of NO_3^--N to N_2O. This is often not the case because denitrification is ubiquitous in natural systems and was deemed to be an important process for removal of NO_3^--N from groundwater (Rivett et al., 2008). For example, Weymann et al. (2008) found denitrification consumed 33–68% of the groundwater NO_3^--N in aquifers contaminated with NO_3^--N. This indicates that the reduction of NO_3^--N in the groundwater should be taken into account when calculating the EF_{5g}. To do this, measurements of initial NO_3^--N concentrations in the groundwater should be included in the calculation of groundwater EF_{5g}.

The Taihu Lake region (TLR) is one of the most intensive agricultural regions in Eastern China and one of the five major rice production regions (Zhu and Chen, 2002). In recent years, more and more paddy fields have been converted to uplands for fruit and vegetable production. With the conversion of land use type, the annual application rate of synthetic N fertilizers has increased from 500 to 600 kg N ha^{-1} for rice-wheat cropping to 900–1300 kg N ha^{-1} for fruit and vegetable production (Hu et al., 2019; Min et al., 2011; Shi et al., 2009; Tian et al., 2007). Large inputs of synthetic N fertilizer have severely disturbed regional N biogeochemical cycling and led to a series of environmental problems, including the eutrophication of surface waters and NO_3^--N pollution of groundwater (Gu et al., 2013). Although it is well known that groundwater NO_3^--N increased rapidly after the conversion of paddy soils to uplands, little is known about its influence on the indirect emissions of N_2O from groundwater and EF_{5g} (Gu et al., 2013; Shi et al., 2009; Xing et al., 2002; Xiong et al., 2006).

During 2015–2017, we measured the spatial and temporal patterns of dissolved N_2O and NO_3^--N concentrations in groundwater under three land-use types with high N-loading in eastern China. The objectives of this study were, (1) to assess the spatial and temporal variability in groundwater N_2O and NO_3^--N concentration under three land-use types in eastern China, and (2) to compare the IPCC EF_{5g} methodology with a proposed improved method using the observed data and other published data. The findings of this study will help focus future N_2O mitigation research on land-uses with high indirect emissions, and will also provide measured data to update EF_{5g} estimates and methods in future IPCC assessments.

2. Materials and methods

2.1. Study sites

The investigations were conducted around the Changshu Agro-ecological Experimental Station (CAS) (31°32′N, 120°41′E) of the Chinese Academy of Sciences in Jiangsu Province. Three arable fields were chosen which represent typical agricultural land-use types in the Taihu lake basin: a paddy field at CAS; a vineyard about 2 km south of CAS; a vegetable field about 1.5 km north of CAS. The vineyard has been used for grape cultivation since 2005 and the vegetable field has been used for vegetable cultivation since 2009. These two sites were paddy fields before their current upland land-use. The soil at all three fields has a silt clay loam texture, was developed from lacustrine sediments, and is classified as Gleyi-Stagnic Anthrosol (CRGCST 2001). The annual mean air temperature in the experimental area is 17.5 °C. Daily rainfall and groundwater level data were recorded at CAS. Rainfall at the sites averaged 1410 mm yr^{-1} during the two-year experimental period (April 2015–April 2017). The management information of the three land-use types were given in Table 1.

2.2. Groundwater monitoring

Groundwater in the surface aquifer was sampled from boreholes manually augured to 1 m depth (local groundwater level) and fitted with a polypropylene random copolymer (PPR) tube (piezometer) of 50-mm inner diameter and 65-mm diameter outer diameter. The piezometer tubes were sealed at the bottom but had several 3 mm-diameter holes drilled in the bottom and covered by a 0.1-mm nylon screen to allow the inflow of filtered groundwater. The tubes extended 0.5 m aboveground and were covered with a removable cap. After installation, the piezometers were pumped dry 5 times over the following 48 h to flush and refill the piezometers. Three piezometers were installed in each different land-use field.

2.3. Groundwater sampling and analysis

Groundwater sampling was carried out bi-monthly from April 2015 to April 2017 using a peristaltic pump (BT100M, Baoding

Table 1
Experimental area, fertilizer N applied and main management practices of the three land-use types.

Land-use type	Field area (ha)	N applied rate (kg N ha^{-1} yr^{-1})	Yearly management practices
Vineyard	3.0	590	March: 15 t ha^{-1} chicken manure (240 kg N ha^{-1}) + 100 kg N ha^{-1} (urea) April: 150 kg N ha^{-1} (urea) May–July: 100 kg N ha^{-1} (urea)
Vegetable Field	5.0	600	October–June: 5 × 120 kg N ha^{-1} (urea, 1 application per crop, 5 crops per year) July–September: no vegetable production due to the high temperature in greenhouse
Paddy Field	4.5	470	Rice: June: 110 kg N ha^{-1} (urea) July: 80 kg N ha^{-1} (urea) August: 80 kg N ha^{-1} (urea) Wheat: November: 80 kg N ha^{-1} (urea) January: 60 kg N ha^{-1} (urea) March: 60 kg N ha^{-1} (urea)

Chuangrui Precision Pump Co. Ltd, China). On the day prior to sampling, all piezometers were pumped dry in order to remove the standing water. On the day of sampling, approximately 200 mL of groundwater was pumped from each piezometer tube into a 100 mL plastic bottle and allowed to overflow the bottle to exclude any ambient air from the being stored in the bottle headspace. The sample was immediately sealed and stored in a refrigerator at 4 °C for the next 2 h.

To determine dissolved N_2O concentration, 5 mL of groundwater sample was injected into a pre-vacuumed 20 mL glass vial (SVF-20 vacuum vials, Nichiden-Rika Glass Co, Ltd, Japan) and ambient air was allowed to flow into the vial to balance barometric pressure. The vial was stored in a refrigerator at 4 °C for 24 h to equilibrate. A 10 mL gas sample was drawn from the vial headspace for the determination of N_2O using an Agilent 7890 gas chromatograph. The concentration of dissolved N_2O was calculated using the equation of Weiss and Price (1980). More details of the measurement process were given in the supporting information (Text S1).

The concentration of NO_3^--N was determined in filtered (cellulose acetate, 0.45 μm) groundwater samples using a SmartChem 140 discrete analyzer (Westco Scientific Instruments) with detection limits of 0.01 mg N L^{-1} for NO_3^--N. All groundwater samples were stored at 4 °C and analysed within 7 days.

Samples collected on 24th February 2017 were used for isotopic analysis of ^{15}N and ^{18}O of NO_3^--N according to the method described by Wang et al. (2015). Firstly, the groundwater NO_3^--N was reduced to nitrite (NO_2^--N) by copper-cadmium particles in a weakly alkaline environment (pH = 8.00 ± 0.02), then the NO_2^--N was further reduced to N_2O by sodium azide in a weakly acidic buffer system (pH = 4.5). The N_2O was then purged from the water sample and trapped cryogenically using an automated system with subsequent release into a gas chromatography column. The isolated N_2O concentration was then analysed with a continuous flow isotope ratio mass spectrometer configured for N and O isotope ratios (Elementar TraceGas-Isoprime100).

2.4. Estimation of N_2O saturation level in groundwater samples

The N_2O saturation level (%) ($N_2O_{(sat)}$) was calculated using Eq. (1).

$$N_2O_{(sat)} = \frac{N_2O_{(gw)}}{N_2O_{(eq)}} \times 100 \quad (1)$$

where $N_2O_{(gw)}$ is the measured N_2O concentration in a groundwater sample, and $N_2O_{(eq)}$ is the N_2O concentration of groundwater in equilibrium with the atmosphere (Weiss and Price, 1980).

2.5. Calculation of the indirect N_2O emission factor (EF_{5g})

The indirect N_2O emission factor (EF_{5g}) was calculated as the ratio between dissolved N_2O and NO_3^--N concentration in groundwater (EF_{5g}(A)) according to the IPCC (2006) method.

$$EF_{5g}\ (A) = \frac{N_2O}{NO_3^- - N} \quad (2)$$

An alternative EF_{5g} (EF_{5g}(B)) (Well et al., 2005) was calculated as,

$$EF_{5g}\ (B) = \frac{N_2O}{NO_3^- - N_{t0}} \quad (3)$$

In this equation, N_2O is the dissolved N_2O concentration in groundwater, NO_3^--N_{t0} is the sum of NO_3^--N + N_2O + excess N_2; and excess N_2 is the N_2 produced by denitrification, which was determined from concentrations of dissolved N_2 and Ar (Böhlke, 2002). The excess N_2 results used in this study were reported previously (Zhou et al., 2018). More details of the determination of groundwater excess N_2 were given in the supporting information (Text S2 and Table S1).

2.6. Statistical analysis

The Shapiro-Wilk test was used to test for homogeneity of variance, and, non-homogeneous data were log-transformed before statistical analysis. Pearson correlation coefficients were used to investigate relationships between NO_3^--N and dissolved N_2O concentrations in the groundwater. Least significant difference (LSD) tests were used to examine differences of groundwater NO_3^--N and dissolved N_2O among different sites. All statistical analyses were performed using SPSS 18.0 version (SPSS Inc., Chicago, IL, USA).

3. Results

3.1. Rainfall and groundwater level over the study period

Daily rainfall and groundwater level were presented in Fig. S1. Annual rainfall was 1344 and 1476 mm during 2015 and 2016. Total rainfall was approximately 10% higher in 2016 than in 2015. Most rainfall occurred during summer. The highest daily rainfall during the experiment was 137 mm on 17 June 2015. Groundwater levels varied in depth from 0.12 to 0.90 m (average = 0.57 m) below the surface over the two-year experiment. Groundwater levels were closer to the surface during summer than in other seasons, due to higher rainfall and irrigation.

3.2. NO_3^--N and dissolved N_2O in groundwater

Average NO_3^--N concentrations in groundwater were 17.6 ± 4.0, 5.6 ± 2.0 and 0.76 ± 0.15 mg N L^{-1} in the vineyard, vegetable and paddy fields, respectively (Fig. 1). NO_3^--N concentrations in groundwater were strongly correlated with land-use type ($P < 0.0001$). There was a clear seasonal variability in NO_3^--N concentration of groundwater under all the three land-use types, with concentrations highest in spring (30.5 ± 8.3, 8.6 ± 2.1, 1.2 ± 0.2 mg N L^{-1} in vineyard, vegetable and paddy fields, respectively) and lowest in autumn (5.1 ± 1.7, 1.9 ± 0.5, 0.4 ± 0.1 mg N L^{-1} in vineyard, vegetable and paddy fields, respectively) (Fig. 2). NO_3^--N concentrations in groundwater were significantly higher in 2015 (24.1 ± 7.1 mg N L^{-1}) than 2016 (10.5 ± 2.7 mg N L^{-1}) under the vineyard ($P < 0.001$), but there were no annual differences observed under vegetable or paddy fields.

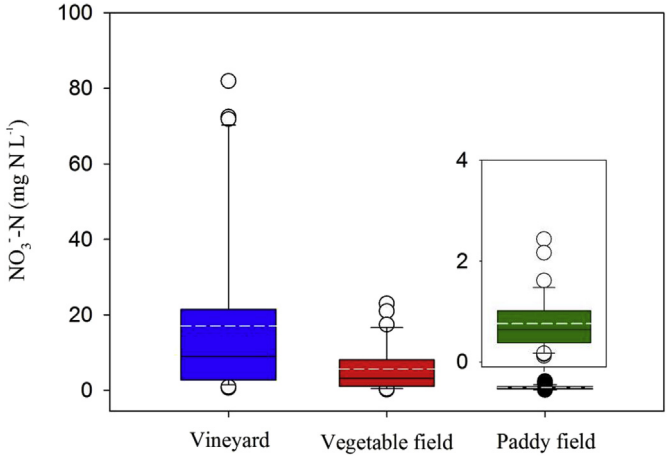

Fig. 1. The distribution of NO_3^--N concentrations in groundwater under the vineyard, vegetable and paddy fields over the two years of observation. The dots, solid center line, dotted line, box extent, and error bars denote the outliers, mean, median, 25th, 75th, 10th, and 90th percentiles, respectively. Note the different scale on the inset box for the paddy field results.

Average N_2O saturation levels were 29,502% (range: 190–221,730%), 9,202% (range: 92–19,489%) and 294% (range: 62–1,554%) in the vineyard, vegetable and paddy fields, respectively. Nearly 99% of N_2O saturation levels exceeded the atmospheric equilibrium, indicating that the groundwater was nearly always a net source of N_2O to the atmosphere (Fig. 4).

The groundwater under the vineyard had the highest dissolved N_2O concentration (average = 58.1 ± 40.4 μg N L^{-1} (Fig. 3). High dissolved N_2O concentrations were also observed in groundwater under the vegetable field (average = 18.5 ± 11.5 μg N L^{-1}), while dissolved N_2O concentrations under the paddy field were much less (average = 0.72 ± 0.27 μg N L^{-1}). Groundwater N_2O concentration was strongly correlated with land-use type ($P < 0.0001$). The maximum concentrations of N_2O in groundwater under vineyard (85.7 ± 20.9 μg N L^{-1}) and vegetable fields (35.7 ± 10.2 μg N L^{-1}) were found in summer and the lowest results occurred in winter (18.4 ± 4.6 and 4.7 ± 1.0 μg N L^{-1}) (Fig. 4). In contrast, groundwater N_2O concentrations in the paddy field were higher during spring (0.85 ± 0.13 μg N L^{-1}) and winter (0.81 ± 0.23 μg N L^{-1}) and lower during autumn (0.50 ± 0.06 μg N L^{-1}). Very high spatial variability of N_2O concentration was observed at all sites, with coefficients of variations of 132%, 93% and 123% in the vineyard, vegetable and paddy fields, respectively.

3.3. Isotopic composition of $\delta^{15}N$ and $\delta^{18}O$ of NO_3^--N

The δ^{15}N-NO_3^--N and δ^{18}O-NO_3^--N values in groundwater are listed in Table 2. The mean values of δ^{15}N-NO_3^--N were 46.5 ± 0.7, 35.3 ± 3.2 and 12.4 ± 4.5‰ in vineyard, vegetable and paddy fields, respectively. The value of δ^{15}N-NO_3^--N was significantly influenced by the land-use type ($P < 0.0001$). The mean values of δ^{18}O-NO_3^--N were 20.6 ± 0.8, 17.3 ± 1.0 and 27.8 ± 4.1‰ in the vineyard,

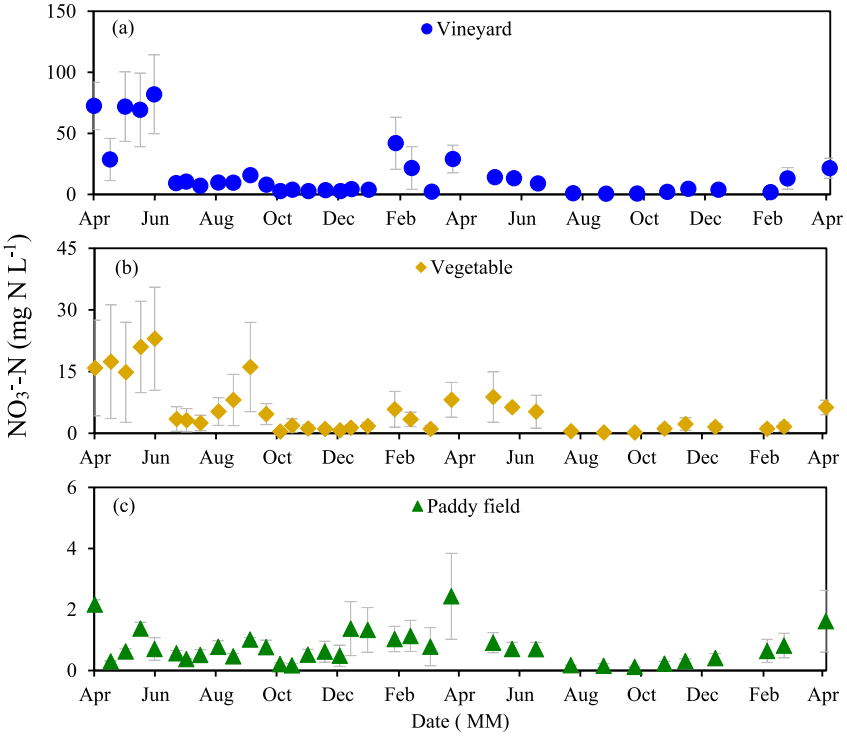

Fig. 2. Temporal variability of NO_3^--N concentration in groundwater under (a) vineyard, (b) vegetable field and (c) paddy field. Error bars represent standard error.

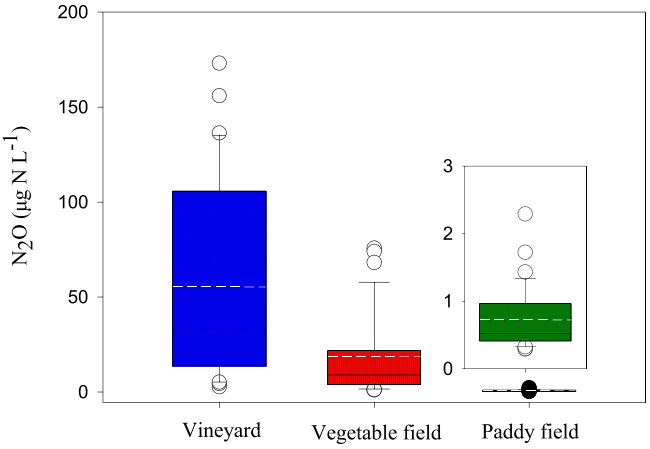

Fig. 3. The distribution of dissolved N_2O concentration results in groundwater under vineyard, vegetable, and paddy fields over the two years of observation. The dots, solid center line, dotted line, box extent, and error bars denote the outliers, mean, median, 25th, 75th, 10th, and 90th percentiles, respectively. Note the different scale on the inset box for the paddy field results.

vegetable and paddy fields, respectively. Only the vegetable and paddy fields were significantly different ($P < 0.0001$).

3.4. Indirect N_2O emission factor (EF_{5g})

The mean values of EF_{5g}(A) were 0.0091, 0.0092 and 0.0019 for the vineyard, vegetable and paddy fields, respectively (Fig. 5). The EF_{5g}(A) of the paddy field was significantly lower than that of the vineyard and vegetable fields ($P < 0.001$). Seasonal variability of EF_{5g}(A) was

Table 2
$\delta^{15}N$ and $\delta^{18}O$ of NO_3^--N in groundwater samples for the three land use types.

Land use type	Fertilizer type	$\delta^{15}N$-NO_3^--N (‰)	$\delta^{18}O$-NO_3^--N (‰)
Vineyard	chicken manure plus urea	46.5 ± 0.7	20.6 ± 0.8
vegetable field	urea	35.3 ± 3.2	17.3 ± 1.0
paddy field	urea	12.4 ± 4.5	27.8 ± 4.0

significant ($P < 0.05$) at all land-use types with EF_{5g}(A) higher during autumn (0.017 ± 0.004, 0.015 ± 0.004, 0.0026 ± 0.0008 in vineyard, vegetable and paddy fields, respectively) and lower during spring (0.0041 ± 0.0016, 0.0058 ± 0.0013, 0.0013 ± 0.0002 in vineyard, vegetable and paddy fields, respectively) (Fig. S2).

The mean values of EF_{5g}(B) were 0.0021, 0.0014 and 0.0007 in the vineyard, vegetable and paddy fields, respectively (Fig. 5). In the vineyard and vegetable fields, EF_{5g}(B) was higher in autumn (0.0032 ± 0.0008 in vineyard) and summer (0.0020 ± 0.0007 in vegetable fields) and lower in winter (0.0011 ± 0.0003 and 0.0010 ± 0.0004). In contrast, EF_{5g}(B) in the paddy field was higher during winter (0.0011 ± 0.0003) and lower in summer (0.0004 ± 0.0001) (Fig. S2).

4. Discussion

4.1. NO_3^--N and dissolved N_2O concentrations in groundwater

The NO_3^--N in groundwater is mainly derived from the leaching of applied N fertilizer, so NO_3^--N concentrations are affected by N application rate and land-use (Di and Cameron, 2002). The concentration of NO_3^--N in the groundwater under flooded rice-

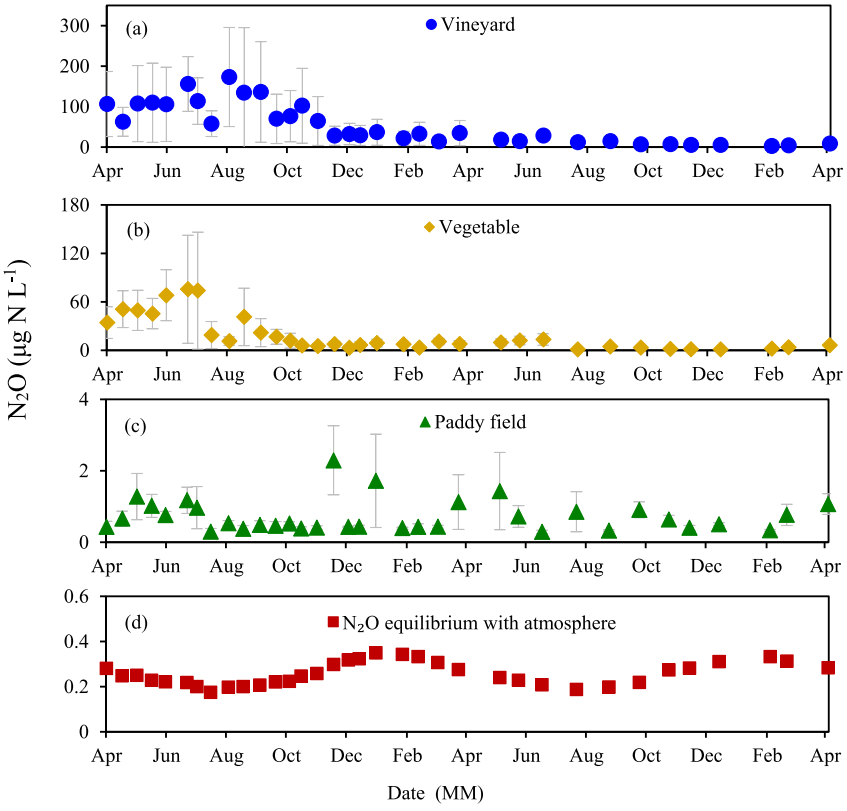

Fig. 4. Temporal variability of groundwater N_2O concentration in (a) vineyard, (b) vegetable field, (c) paddy field and (d) N_2O equilibrium with atmosphere. Error bars represent standard error.

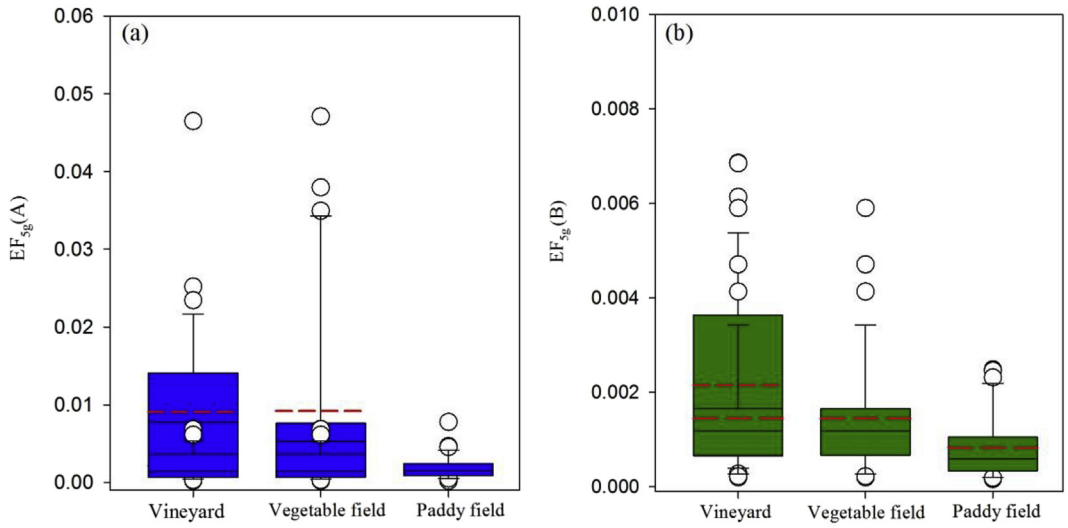

Fig. 5. The distribution of (a) EF_{5g}(A) and (b) EF_{5g}(B) of vineyard, vegetable, and paddy fields over the two years of observation. The dots, solid center line, dotted line, box extent, and error bars denote the outliers, mean, median, 25th, 75th, 10th, and 90th percentiles, respectively.

growing paddy soils is typically low due to the high denitrification activity in the anaerobic surface soil which reduced the amount of NO_3^--N available for leaching (Tian et al., 2007). In contrast, the surface soil of upland vineyard and vegetable fields was well-drained, promoted nitrification rather than denitrification, and led to leaching of NO_3^--N through the soil into the groundwater below (Zhou et al., 2016).

In the vineyard and vegetable fields of this study, the difference in groundwater NO_3^--N concentrations can be attributed to the different fertilization practices used. In the vineyard, 240 kg ha^{-1} of organic N plus 100 kg N ha^{-1} of fertilizer N was applied as basal fertilizer in March, with another 250 kg ha^{-1} fertilizer N applied over the next three months (Table 1). These high N applications, combined with precipitation after fertilization, resulted in NO_3^--N leaching into the groundwater, especially when the N input exceeded the demand of the crops in spring (Di and Cameron, 2002). However, in the vegetable field, the 600 kg N ha^{-1} applied was split into five applications of 120 kg N ha^{-1} according to the vegetable management regime. In this case the temporal variability in groundwater NO_3^--N was less pronounced compared with the vineyard. Furthermore, since N fertilization and irrigation were more frequent in spring and summer because of the rapid growth of the vegetables and the higher temperature compared with winter, higher concentrations of NO_3^--N in the groundwater were measured in spring and summer, and lower concentrations observed in winter.

Many processes such as nitrification, denitrification and nitrifier-denitrification can produce N_2O, so it can be difficult to identify the source of N_2O in groundwater. The microbial processes of nitrification and denitrification trigger isotopic fractionation causing alterations of the $\delta^{15}N$ and $\delta^{18}O$ of the NO_3^--N. Usually the conversion of NH_4^+-N to NO_2^--N and NO_3^--N is accompanied by marked N-isotope fractionation, resulting in NO_3^--N that is depleted in $\delta^{15}N$ relative to the $\delta^{15}N$ of the initial NH_4^+-N. In contrast, denitrification will enrich the $\delta^{15}N$ and $\delta^{18}O$ of the residual NO_3^--N, with an enrichment factor of −40 to −5‰ for $\delta^{15}N$ and −18‰ to −8‰ for $\delta^{18}O$ (Xue et al., 2009).

In present study, the NO_3^--N in groundwater originated from mineralized soil organic matter and applied organic and inorganic N fertilizers. Organic fertilisers, such as chicken manure, usually have a higher $\delta^{15}N$ (18–25‰) than urea (-6–6‰) (Xing et al., 2002; Xue et al., 2009). Both chicken manure and urea were applied to the vineyard soil, so the $\delta^{15}N$ of the NO_3^--N in groundwater below the vineyard should range from -6–25‰. However, the measured $\delta^{15}N$ (46.5‰) was far greater than expected (Table 2). Similar results were also observed for the vegetable and paddy fields. The observed enrichment of $\delta^{15}N$ and $\delta^{18}O$ in the NO_3^--N of groundwater samples in our study was strong evidence to support denitrification as the dominant N_2O production process in the groundwater of the studied fields (Table 2).

In the present study, the dissolved N_2O concentrations in groundwater under the vineyard (range: 2.6–234 μg N L^{-1}) and vegetable fields (range: 1.1–76 μg N L^{-1}) were similar to those previously observed in upland soils, while the dissolved N_2O concentrations under the paddy field (range: 0.3–2.3 μg N L^{-1}) were similar to other work done in wetlands (Table 3). In general, the N_2O concentrations in groundwater below vineyard and vegetable fields were almost an order of magnitude higher than those in the paddy field. The influence of land-use type on groundwater N_2O concentration has also been reported from studies in Germany (Von der Heide et al., 2008) and Britain (Jurado et al., 2017). N_2O concentrations in groundwater were generally higher under arable land than under grassland, forest areas or natural wetlands because the higher rates of N fertilizer use on arable land increased NO_3^--N in the soil and groundwater (Table 3). However, high concentrations of N_2O in groundwater have also been observed in grassland and forest areas with either nil or low N input (Jahangir et al., 2013; Koba et al., 2009; Mander et al., 2014; McAleer et al., 2017), which indicated that groundwater N_2O could be affected by factors other than N fertilizer application. The high spatial and temporal variations of groundwater N_2O concentration observed in the present study were typical of previous reports of this measurement conducted elsewhere (Gardner et al., 2016; Von der Heide et al., 2008; Weymann et al., 2008).

4.2. Indirect N_2O emission factor

According to the IPCC (2006) method, the EF_{5g}(A) is calculated as the ratio between dissolved N_2O and NO_3^--N concentration in groundwater. This calculation assumes that the NO_3^--N and N_2O are not transformed during transport from groundwater to watershed areas, which is unlikely to be the case. The EF_{5g}(A) of the paddy field (0.0019) in our study was comparable to the values reported by Zhou et al. (2017) (0.001–0.006) and Xiong et al. (2006) (0.0011).

Table 3
NO_3^--N, N_2O, excess N_2, EF_{5g}(A) and EF_{5g}(B) in different land use types.

Land use types	NO_3^--N (mg N L^{-1})	Excess N_2 (mg N L^{-1})	N_2O (μg N L^{-1})	EF_{5g}(A)	EF_{5g}(B)	Reference
Natural wetland	0.06	2.75	3.92	0.0718	0.0014	Fox et al. (2014)
Natural wetland	0.05	2.59	3.36	0.0747	0.0013	Fox et al. (2014)
Natural wetland	2.60	3.47	132.1	0.0508	0.0213	Mookherji et al. (2003)
Riparian buffer	4.58	1.69	16.80	0.0037	0.0027	Fox et al. (2014)
Riparian buffer	0.68	4.90	4.20	0.0062	0.0008	Fox et al. (2014)
Riparian buffer	1.71	3.01	4.80	0.0028	0.0010	Mander et al. (2014)
Riparian buffer	0.16	2.43	0.52	0.0033	0.0002	Mander et al. (2014)
Grassland	0.93	2.28	24.00	0.0257	0.0074	Jahangir et al. (2013)
Grassland	0.38	2.33	11.00	0.0286	0.0040	Jahangir et al. (2013)
Grassland	9.80	0.40	12.10	0.0012	0.0012	McAleer et al. (2017)
Grassland	0.30	2.40	1.10	0.0036	0.0004	McAleer et al. (2017)
Cropland	8.51	4.20	89.00	0.0108	0.0070	Weymann et al. (2008)
Cropland	9.26	2.08	8.27	0.0025	0.0007	Weymann et al. (2008)
Cropland	4.89	7.97	18.39	0.0037	0.0014	Weymann et al. (2008)
Cropland	3.84	3.19	3.40	0.0009	0.0005	Weymann et al. (2008)
Cropland	8.64	0.90	38.00	0.0044	0.0040	Jahangir et al. (2013)
Cropland	14.85	0.46	49.00	0.0033	0.0032	Jahangir et al. (2013)
Cropland	5.99	2.32	13.16	0.0022	0.0016	Fox et al. (2014)
Cropland	0.31	5.67	0.65	0.0440	0.0001	Gardner et al. (2016)
Cropland	7.50	0.87	6.57	0.0009	0.0008	McAleer et al. (2017)
Cropland	7.60	0.80	2.60	0.0003	0.0003	McAleer et al. (2017)
Vineyard	17.63	11.20	58.12	0.0091	0.0021	This study
Vegetable field	5.59	5.70	18.51	0.0092	0.0014	This study
Paddy field	0.76	0.80	0.72	0.0019	0.0007	This study
Average	–	–	–	0.0152	0.0027	

These low values indicate that the paddy soil contributed minimal N_2O through indirect emissions to the atmosphere. The EF_{5g}(A) of the vineyard (0.0091) and vegetable (0.0092) fields were much higher than the IPCC default value (0.0025), indicating that these land-uses may be important sources of indirect atmospheric N_2O emissions. Similar to our results, other research conducted in China also found EF_{5g}(A) of upland areas was higher than the IPCC (2006) default value (Tian et al., 2018; Yan et al., 2012; Yu et al., 2013). Tian et al. (2019) summarized the EF_{5g}(A) values from the literature and found the average value (0.0060) to be twice as high as the default value (0.0025).

The default IPCC EF_{5g}(A) value was derived from only a few studies available at the time (IPCC, 2006). The large differences between this default value and much of the measured data since 2006 undermines its credibility for use in scaling of indirect N_2O emissions to regional, national and global scales. Therefore, the default EF_{5g}(A) value should be revised in the light of new research that better encompasses regional variability in soil types, land-use types and N fertilizer rates (Tian et al., 2019).

For instance, Fox et al. (2014) reported very high values of EF_{5g}(A) (0.072–0.075) in natural wetlands and identified them as hotspots for indirect N_2O emission. However, aquifers below natural wetlands or riparian buffer zones typically have groundwater N_2O concentration in equilibrium with the atmosphere, so they are unlikely to be a significant source of indirect N_2O emissions (Jurado et al., 2017). Measured indirect N_2O emissions from such aquifers are often minimal and these areas could even be a sink, rather than a source of indirect N_2O emission (Audet et al., 2014; Moseman-Valtierra et al., 2011; Weymann et al., 2009). Although N_2O and NO_3^--N concentrations in the groundwater may be low, the ratio between the two components can still indicate the potential for large indirect N_2O emissions from the groundwater, even though the reality is likely to be the opposite (Table 3).

In addition to the large uncertainty around the current default EF_{5g}(A), the calculation method also presented some conceptual limitations in estimating indirect N_2O emissions as it assumed that aquatic systems acted solely as a transport mechanism without any further processing of NO_3^--N and N_2O. However, the production and reduction of NO_3^--N and N_2O did continue to occur during the transport of groundwater to adjacent surface water bodies (Zhou et al., 2018). Therefore, the reduction of NO_3^--N in the groundwater should be taken into account when calculating the indirect N_2O emission factor, which was otherwise erroneous in its description of real-world processes.

As an alternative, Well et al. (2005) proposed an alternative method to improve the calculation of the indirect N_2O emission factor from groundwater (EF_{5g}(B)). In the alternative method, excess N_2 measured in the sample was assumed to represent the NO_3^--N consumed by denitrification. In this way, the initial, not the residual, NO_3^--N concentration was taken into account when calculating EF_{5g}. In the present study, the EF_{5g}(A) results were 3–5 times higher than those of EF_{5g}(B). A similar trend was also found by other researchers who have calculated both EF_{5g}(A) and EF_{5g}(B) (Table 3). Largest differences between EF_{5g}(A) and EF_{5g}(B) were observed in aquifers with high denitrification activity (Gardner et al., 2016; Jahangir et al., 2013; Mander et al., 2014). For example, the EF_{5g}(A) was 50 times higher than EF_{5g}(B) in a natural wetland where more than 95% of the leached NO_3^--N was consumed by denitrification (Fox et al., 2014). Conversely, only small differences between EF_{5g}(A) and EF_{5g}(B) were observed in areas where groundwater denitrification activity was low (McAleer et al., 2017; Well et al., 2005). Interestingly, the average EF_{5g}(A) value (0.0152) approximated the initial default value (0.015) published by IPCC (1997), while the average EF_{5g}(B) (0.0027) approximated the reduced default value of 0.0025 in IPCC (2006). Furthermore, EF_{5g}(B) better described the relationship between the indirect N_2O emission factor and dissolved N_2O concentration (Fig. 6). Therefore, we propose that the EF_{5g}(B) methodology is the more scientifically appropriate measurement for calculating the indirect N_2O emission factor from groundwater.

5. Conclusion

Large uncertainly still exists about the quantum of indirect N_2O emissions from agricultural systems because limited observational data of EF_{5g} is available, especially for high N-loading farmlands. In the present study, we investigated the dissolved N_2O concentration and EF_{5g} under three land-use types with high N inputs located in

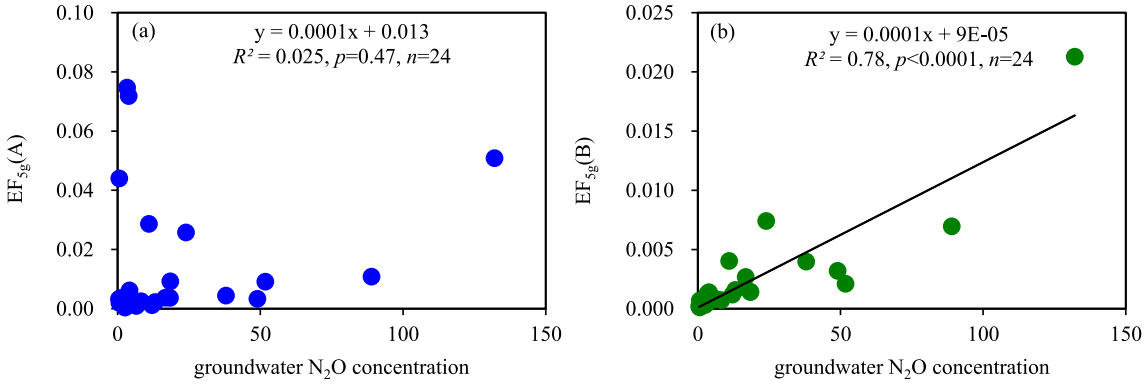

Fig. 6. Regression analyses of N_2O concentration in groundwater with (a) $EF_{5g}(A)$ and (b) $EF_{5g}(B)$ in different land use types.

eastern China. In two years of observation, almost 99% groundwater samples exhibited N_2O saturation levels exceeding the atmospheric equilibrium, indicating that the groundwater in all three land-use systems was a net source of N_2O to the atmosphere.

Land-use strongly influenced the N_2O present in groundwater, with much less present in the groundwater under the irrigated rice paddy than under the upland vineyard or vegetable fields. Calculated indirect N_2O emission factors indicated that the paddy soil contributed minimal indirect N_2O emission to the atmosphere while the vegetable and vineyard field can be important sources of indirect N_2O emission. We found indirect N_2O emissions to be both spatially heterogenerous and temporally variable. Therefore, more observations of indirect N_2O emission are needed to improve the reliability and confidence of this potentially important source of greenhouse gas emissions from high N-loading farming systems.

Our comparisons of the default N_2O indirect emission factor methodology with an improved calculation demonstrated that the current default method may overestimate the contribution of groundwater N_2O to the global N cycle because it does not consider the role of denitrification in reducing groundwater NO_3^--N. This overestimation was most pronounced in aquifers with high denitrification activity. The improved method provides a more scientifically appropriate measure of the indirect emission of N_2O from groundwater.

Acknowledgments

This study was financially supported by the National Key Research and Development Program of China (2017YFD0200100, 2018YFD0201200), the National Natural Science Foundation of China (41425005, 41807096), and Joint Sino-German Research Project (GZ1262).

Appendix A. Supplementary data

Supplementary data to this article can be found online at https://doi.org/10.1016/j.envpol.2019.02.027.

References

Audet, J., Hoffmann, C.C., Andersen, P.M., Baattrup-Pedersen, A., Johansen, J.R., Larsen, S.E., Kjaergaard, C., Elsgaard, L., 2014. Nitrous oxide fluxes in undisturbed riparian wetlands located in agricultural catchments: emission, uptake and controlling factors. Soil Biol. Biochem. 68, 291–299.
Böhlke, J.K., 2002. Groundwater recharge and agricultural contamination. Hydrogeol. J. 10, 153–179.
Cooper, R.J., Wexler, S.K., Adams, C., Hiscock, K.M., 2017. Hydrogeological controls on regional-scale indirect nitrous oxide (N_2O) emission factors for rivers. Environ. Sci. Technol. 51 (18), 10440–10448.
CRGCST (Cooperative Research Group on Chinese Soil Taxonomy), 2001. Chinese Soil Taxonomy. Science Press, Beijing and New York, pp. 166–167.
Di, H., Cameron, K., 2002. Nitrate leaching in temperate agroecosystems: sources, factors and mitigating strategies. Nutrient Cycl. Agroecosyst. 64, 237–256.
Fox, R., Fisher, T., Gustafson, A., Jordan, T., Kana, T., Lang, M., 2014. Searching for the missing nitrogen: biogenic nitrogen gases in groundwater and streams. J. Agric. Sci. 152, 96–106.
Gardner, J.R., Fisher, T.R., Jordan, T.E., Knee, K.L., 2016. Balancing watershed nitrogen budgets: accounting for biogenic gases in streams. Biogeochemistry 127, 231–253.
Gu, B., Ge, Y., Chang, S.X., Luo, W., Chang, J., 2013. Nitrate in groundwater of China: sources and driving forces. Glob. Environ. Chang. 23, 1112–1121.
Hasegawa, K., Hanaki, K., Matsuo, T., Hidaka, S., 2000. Nitrous oxide from the agricultural water system contaminated with high nitrogen. Chemosphere Global Change Sci. 2, 335–345.
Hu, Z., Towfiqul Islam, A.R.M., Chen, S., Hu, B., Shen, S., Wu, Y., Wang, Y., 2019. Effects of warming and reduced precipitation on soil respiration and N_2O fluxes from winter wheat-soybean cropping systems. Geoderma 337, 956–964.
IPCC, 1997. Greenhouse gas emissions from agricultural soils. In: Houghton, J.T., et al. (Eds.), Greenhouse Gas Inventory Reference Manual. Revised 1996 IPCC Guidelines for National Greenhouse Gas Inventories. IPCC/OECD/IES. UK Meteorological Office, Bracknell, UK.
IPCC, 2006. 2006 IPCC Guidelines for National Greenhouse Gas Inventories.
Jahangir, M.M., Johnston, P., Barrett, M., Khalil, M.I., Groffman, P.M., Boeckx, P., Fenton, O., Murphy, J., Richards, K.G., 2013. Denitrification and indirect N_2O emissions in groundwater: hydrologic and biogeochemical influences. J. Contam. Hydrol. 152, 70–81.
Jahangir, M.M.R., Johnston, P., Khalil, M.I., Hennessy, D., Humphreys, J., Fenton, O., Richards, K.G., 2012. Groundwater: a pathway for terrestrial C and N losses and indirect greenhouse gas emissions. Agric. Ecosyst. Environ. 159, 40–48.
Jurado, A., Borges, A.V., Brouyere, S., 2017. Dynamics and emissions of N_2O in groundwater: a review. Sci. Total Environ. 584–585, 207–218.
Koba, K., Osaka, K., Tobari, Y., Toyoda, S., Ohte, N., Katsuyama, M., Suzuki, N., Itoh, M., Yamagishi, H., Kawasaki, M., Kim, S.J., Yoshida, N., Nakajima, T., 2009. Biogeochemistry of nitrous oxide in groundwater in a forested ecosystem elucidated by nitrous oxide isotopomer measurements. Geochem. Cosmochim. Acta 73, 3115–3133.
Ma, Y., Schwenke, G., Sun, L., Liu, D.L., Wang, B., Yang, B., 2018. Modeling the impact of crop rotation with legume on nitrous oxide emissions from rain-fed agricultural systems in Australia under alternative future climate scenarios. Sci. Total Environ. 630, 1544–1552.
Mander, U., Well, R., Weymann, D., Soosaar, K., Maddison, M., Kanal, A., Lõhmus, K., Truu, J., Augustin, J.r., Tournebize, J., 2014. Isotopologue ratios of N_2O and N_2 measurements underpin the importance of denitrification in differently N-loaded riparian alder forests. Environ. Sci. Technol. 48, 11910–11918.
McAleer, E.B., Coxon, C.E., Richards, K.G., Jahangir, M.M., Grant, J., Mellander, P.E., 2017. Groundwater nitrate reduction versus dissolved gas production: a tale of two catchments. Sci. Total Environ. 586, 372–389.
Min, J., Zhao, X., Shi, W., Xing, G., Zhu, Z., 2011. Nitrogen balance and loss in a greenhouse vegetable system in southeastern China. Pedosphere 21, 464–472.
Mookherji, S., McCarty, G.W., Angier, J.T., 2003. Disssolved gas analysis for assessing the fate of nitrate in wetlands. J. Am. Water Resource. 39, 381–387.
Moseman-Valtierra, S., Gonzalez, R., Kroeger, K.D., Tang, J., Chao, W.C., Crusius, J., Bratton, J., Green, A., Shelton, J., 2011. Short-term nitrogen additions can shift a coastal wetland from a sink to a source of N_2O. Atmos. Environ. 45, 4390–4397.
Myhre, G., Shindell, D., Bréon, F.-M., Collins, W., Fuglestvedt, J., Huang, J., Koch, D., Lamarque, J., Lee, D., Mendoza, B., Nakajima, T., Robock, A., Stephens, G., Takemura, T., H. Z, 2013. Anthropogenic and natural radiative forcing. In: Stocker, T.F., Qin, D., Plattner, G.-K., et al. (Eds.), Climate Change 2013: the Physical Science Basis. Contribution of Working Group I to the Fifth Assessment. Report of the Intergovernmental Panel on Climate Change. Cambridge University Press, Cambridge, United Kingdom and New York, NY, USA.
Ravishankara, A., Daniel, J.S., Portmann, R.W., 2009. Nitrous oxide (N_2O): the

dominant ozone-depleting substance emitted in the 21st century. Science 326, 123–125.
Reay, D.S., Davidson, E.A., Smith, K.A., Smith, P., Melillo, J.M., Dentener, F., Crutzen, P.J., 2012. Global agriculture and nitrous oxide emissions. Nat. Clim. Change 2, 410.
Reay, D.S., Smith, K.A., Edwards, A.C., 2003. Nitrous oxide emission from agricultural drainage waters. Glob. Chang. Biol. 9, 195–203.
Rivett, M.O., Buss, S.R., Morgan, P., Smith, J.W., Bemment, C.D., 2008. Nitrate attenuation in groundwater: a review of biogeochemical controlling processes. Water Res. 42, 4215–4232.
Shi, W., Yao, J., Yan, F., 2009. Vegetable cultivation under greenhouse conditions leads to rapid accumulation of nutrients, acidification and salinity of soils and groundwater contamination in South-Eastern China. Nutrient Cycl. Agroecosyst. 83, 73–84.
Stocker, T., 2014. Climate Change 2013: the Physical Science Basis: Working Group I Contribution to the Fifth Assessment Report of the Intergovernmental Panel on Climate Change. Cambridge University Press.
Syakila, A., Kroeze, C., 2011. The global nitrous oxide budget revisited. Greenh. Gas Meas. Manag. 1, 17–26.
Tian, L., Akiyama, H., Zhu, B., Shen, X., 2018. Indirect N_2O emissions with seasonal variations from an agricultural drainage ditch mainly receiving interflow water. Environ. Pollut. 242, 480–491.
Tian, L., Cai, Y., Akiyama, H., 2019. A review of indirect N_2O emission factors from agricultural nitrogen leaching and runoff to update of the default IPCC values. Environ. Pollut. 245, 300–306.
Tian, Y., Yin, B., Yang, L., Yin, S., Zhu, Z., 2007. Nitrogen runoff and leaching losses during rice-weat rotations in Taihu Lake region, China. Pedosphere 17, 445–456.
Von der Heide, C., Böttcher, J., Deurer, M., Weymann, D., Well, R., Duijnisveld, W., 2008. Spatial variability of N_2O concentrations and of denitrification-related factors in the surficial groundwater of a catchment in Northern Germany. J. Hydrol. 360, 230–241.
Wang, X., Cao, Y., Han, Y., Tang, H., Wang, R., Sun, X., Sun, Y., 2015. Determination of nitrogen and oxygen isotope ratio of nitrate in water. Acta Pedol. Sin. 52, 558–566.
Weiss, R., Price, B., 1980. Nitrous oxide solubility in water and seawater. Mar. Chem. 8, 347–359.
Well, R., Weymann, D., Flessa, H., 2005. Recent research progress on the significance of aquatic systems for indirect agricultural N_2O emissions. Environ. Sci. 2, 143–151.
Weymann, D., Well, R., Flessa, H., Von der Heide, C., Deurer, M., Meyer, K., Konrad, C., Walther, W., 2008. Groundwater N_2O emission factors of nitrate-contaminated aquifers as derived from denitrification progress and N_2O accumulation. Biogeosciences 5, 1215–1226.
Weymann, D., Well, R., von der Heide, C., Böttcher, J., Flessa, H., Duijnisveld, W.H.M., 2009. Recovery of groundwater N_2O at the soil surface and its contribution to total N_2O emissions. Nutrient Cycl. Agroecosyst. 85, 299–312.
Xing, G., Cao, Y., Shi, S.L., Sun, G.Q., Du, L.J., Jianguo, Z., 2002. Denitrification in underground saturated soil in a rice paddy region. Soil Biol. Biochem. 34, 1593–1598.
Xiong, Z.Q., Xing, G.X., Zhu, Z.L., 2006. Water dissolved nitrous oxide from paddy agroecosystem in China. Geoderma 136, 524–532.
Xue, D., Botte, J., De Baets, B., Accoe, F., Nestler, A., Taylor, P., Van Cleemput, O., Berglund, M., Boeckx, P., 2009. Present limitations and future prospects of stable isotope methods for nitrate source identification in surface- and groundwater. Water Res. 43, 1159–1170.
Yan, W., Yang, L., Wang, F., Wang, J., Ma, P., 2012. Riverine N_2O concentrations, exports to estuary and emissions to atmosphere from the Changjiang River in response to increasing nitrogen loads. Glob. Biogeochem. Cycles 26 (n/a-n/a).
Yu, Z., Deng, H., Wang, D., Ye, M., Tan, Y., Li, Y., Chen, Z., Xu, S., 2013. Nitrous oxide emissions in the Shanghai river network: implications for the effects of urban sewage and IPCC methodology. Glob. Chang. Biol. 19, 2999–3010.
Zhou, J., Gu, B., Schlesinger, W.H., Xiaotang, J., 2016. Significant accumulation of nitrate in Chinese semi-humid croplands. Sci. Rep. 6, 25088.
Zhou, W., Ma, Y., Well, R., Wang, H., Yan, X., 2018. Denitrification in shallow groundwater below different arable land systems in a high nitrogen-loading region. J. Geophys. Res.: Biogeosciences 123, 991–1004.
Zhou, W., Xia, L., Yan, X., 2017. Vertical distribution of denitrification end-products in paddy soils. Sci. Total Environ. 576, 462–471.
Zhu, Z., Chen, D., 2002. Nitrogen fertilizer use in China–Contributions to food production, impacts on the environment and best management strategies. Nutrient Cycl. Agroecosyst. 63, 117–127.